

UNIVERSITATEA „POLITEHNICA” of BUCHAREST



PhD THESIS

Summary

OPTO-ELECTRONIC COMMAND AND CONTROL SYSTEMS FOR ULTRA-INTENS LASERS

Supervisor: PhD. Prof. Eng. Paul Șchiopu

PhD student: Eng. Mihai Șerbănescu

BUCHAREST 2020

**OPTO-ELECTRONIC COMMAND AND CONTROL
SYSTEMS FOR ULTRA-INTENS LASERS**

Acknowledgments

The realization of the present thesis was possible with the total support of Prof. Dr. Eng. Paul Șchiopu, the supervisor of the doctoral thesis, as well as the entire guidance team: Prof. Dr. Eng. Adrian Manea, Prof. Dr. Eng. Marian Vladescu and Prof. Dr. Eng. Ioan Plotog, to whom I would like to express my sincere gratitude for all the support they offered to me throughout the doctoral school period. During the elaboration of this thesis, I benefited from the permanent support from Dr. Marian Zamfirescu, Head of CETAL, whom I want to especially thank.

I would like to thank my colleagues Dr. Săndel Simion, Dr. Andreea Groza, Dr. Cătălin Luculescu, and Dr. Liviu Neagu for their guidance, suggestions, and support in the elaboration of this thesis.

I would like to especially thank my colleagues from the CETAL-PW team, Dr. Achim Alexandru, Dr. Aurelian Marcu, Dr. Constantin Diplășu, Dr. Georgiana Giubega, Dr. Răzvan Ungureanu and Dr. Gabriel Cojocaru for their requirements related to the CETAL-PW laser system, for their help, suggestions, and criticisms regarding the implemented solutions. They have influenced and contributed decisively to the results presented in this paper.

Last but not least, I would like to thank my family for their support and understanding throughout doctoral studies.

Contents

1. Introduction	1
2. Command and control of ultra-intense lasers	2
2.1 Introduction	2
2.2 Synchronization stage.....	3
2.3 Chronometer stage.....	4
2.4 Optical path correction.....	6
3. CETAL-PW laser system	8
4. Implementation of the adopted solutions	10
4.1 Introduction	10
4.2 Synchronization system – SINCROLASER.....	10
4.3 Temporal monitoring system of optical pulses from ultra-intense lasers.....	15
4.4 Beam position control system for CETAL PW laser	23
5. Applications of developed solutions in laser scanning	26
6. Conclusions	28
Bibliography	29

Note: The bibliographic references was kept from PhD Thesis;

1. Introduction

The laser is one of the greatest inventions of mankind that allows the guidance and control of light in order to use it in modern world applications. The permanent increase of the output power was limited by the damage threshold of the optical components used, respectively by reaching the threshold of energy density transmitted both spatially and temporally.

Overcoming this obstacle was made possible by an original approach by Professor Gérard Mourou together with Donna Strickland. They proposed a global system of amplification of laser pulses by their temporal expansion, the actual amplification and their recompression, a method called "Chirped Pulse Amplification" (CPA) [1].

This technology has made it possible to obtain laser beams with peak powers of the order of 10 PW, a technology currently implemented at the ELI-NP facility, which hosts a laser system with two 10 PW parallel outputs controlled by a common front-end [2].

Increasing this peak power is possible by using laser amplifiers arranged in parallel [3] and then coherently combining the beams on the target [4]. Another approach is OPCPA ("Optical Parametric Chirped Pulse Amplification") [5]. This is a second-order nonlinear process generated by the spatial and temporal overlapping of two laser beams which generates a new wave with a frequency equal to the difference of the initial wave frequencies. Basically, there is an amplification of the signal beam during the spatial and temporal overlapping of the respective waves. The temporal overlapping of laser pulses involves synchronization elements as well as their measurement and control systems. With this technique it is possible to directly obtain 100 PW laser pulses [6].

This paper follows an original method for generating solutions for ultra-high intensity lasers such as synchronization, temporal and spatial control for laser pulses for OPCPA amplifier parameters to create higher intensities for future 100 PW laser systems and with immediate applications for the existing 1 PW and 10 PW CPA lasers.

Thus, the original research conducted during this thesis was tested and implemented directly within the National Institute for Laser, Plasma and Radiation Physics (INFLPR) where the ultra-intense CETAL-PW laser was installed, used and developed and it can ensure maximum laser pulses of 1 PW ($1 \text{ PW} = 10^{15} \text{ W}$). The functional tests and the operation of the CETAL-PW laser demonstrated the need to adopt the researched solutions for the implementation of command and control systems, both for the maintenance of the optical path and also for the temporal control.

The thesis includes the research, the design and sizing details of the proposed systems, their physical implementation and their testing in the real framework of CETAL-PW laser operation. Basically, in the second chapter there are analyzed the ultra-intense lasers, both those in the range 1 PW-10 PW amplified by the CPA technique ("Chirped Pulse Amplification") and the future ones in the range of 100 PW amplified by the OPCPA technique ("Optical Parametric Chirped Pulse Amplification"), in terms of command and

control systems. The implementable solutions as well as the innovative solutions developed in the thesis are presented.

Chapter 3 presents the CETAL-PW laser, highlighting the initial command and control blocks both in terms of space and time, as well as their limitations.

Chapter 4 presents the complete implementation of the proposed solutions for both temporal control elements (synchronization stage, temporal monitoring stage of laser pulses) and spatial ones by monitoring the position of the laser beam as it moves through the transport system. Chapter 5 additionally presents an implementation of the concepts developed in the thesis and applied in a practical LIDAR laser scanning project with applications in the automotive industry.

The annexes present the programs used to control the equipment developed in the thesis, both the internal programs written in assembly language and the computer interface programs written in python.

2. Command and control of ultra-intense lasers

2.1. Introduction

For the operation within optimal parameters of ultra-intense lasers both for those in the range of 1 PW-10 PW amplified with CPA ("Chirped Pulse Amplification") technique and the future ones amplified in the range of 100 PW amplified with OPCPA ("Optical Parametric Chirped Pulse Amplification") time synchronizations as well as optical paths are critical. Any desynchronization will generate the elimination of the optical pulse amplification and any optical path error will generate either the destruction of the optical elements present on its path or the destruction of the pulse itself. The block diagram of a super-intense laser, in terms of commands and control is shown in Fig.2.1:

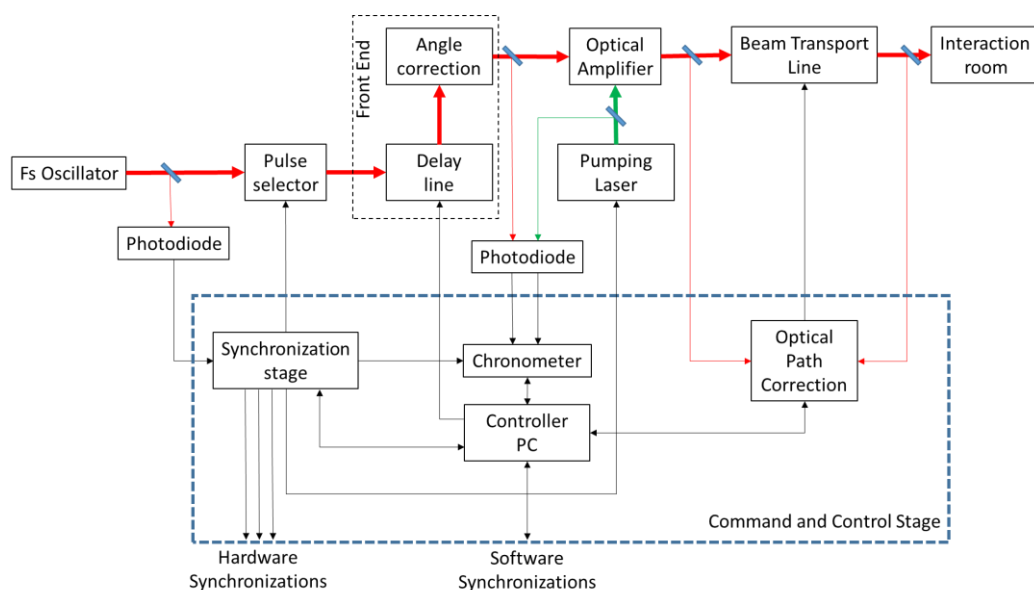


Fig.2.1. Block diagram of ultrashort pulse amplification with CPA and OPCPA techniques

Figure 2.1 shows the simplified optical chain, respectively the femtosecond oscillator, the pulse selector, the beam conditioning stage for the OPCPA lasers for controlling the direction and time to be travelled, the optical amplifier and the laser beam transport line to the interaction chamber.

The command and control for a super-intense laser system must contain:

- A synchronization stage that ensures the control of pumping lasers and the selection of useful laser pulses by means of electro-optical modulators (Pockels cells) for low energies and small beam diameters and opto-mechanical switches for large beam diameters and low working frequencies or in pulse by pulse work regimes;
- A stage for measuring the time intervals between the useful laser pulse and the pump pulse(s) for maximum optical amplification;
- A system for detecting and correcting the optical path through the laser system and through the transport system of the beam to the interception chamber.

2.2. Synchronization stage

The role of this stage is to ensure the selection of the pulses and the control of all the active elements in the laser as well as all the external synchronizations correlated with the laser pulse.

The block diagram of a synchronization stage is shown in fig.2.2:

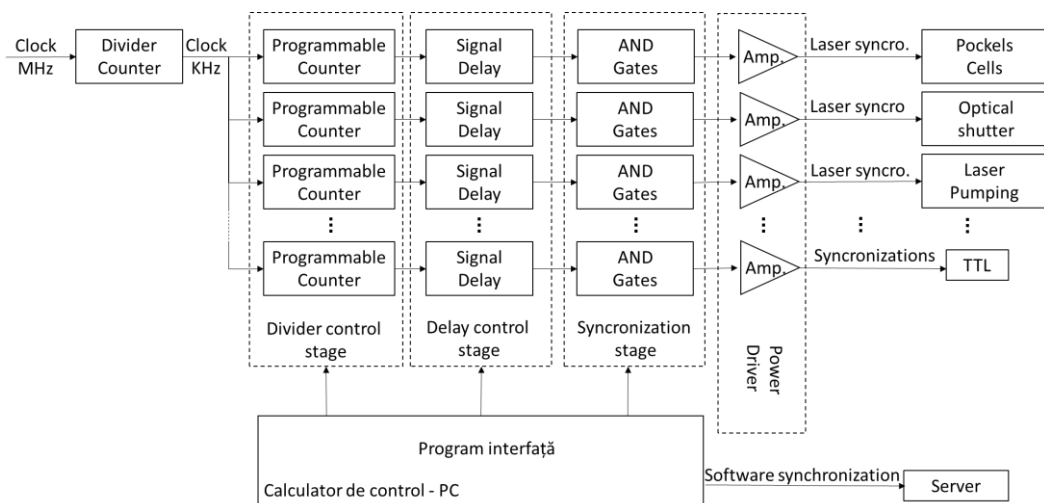


Fig.2.2. Block diagram of the synchronization stage for ultra-intense lasers

It consists of a fixed frequency divider that provides the kHz frequency system clock (usually 1 kHz) from the generic MHz frequency clock synchronous with the laser pulses generated by the femtosecond optical oscillator.

The kHz system clock is decreased by synchronous programmable counters at the required laser operating frequencies, respectively 1 kHz, 100 Hz, 10 Hz, 1 Hz, 0.1 Hz, etc. Since each new clock obtained controls an active element of the super-intense laser, a programmable pulse delay stage is also required to synchronize the execution of the respective command with the optical pulse.

The control thus obtained must be conditioned by the overall operating mode of the laser, i.e. continuous pulses, burst or pulse by pulse and finally amplified specifically for the control of the execution stage: electro-optical switches (Pockels cells and acousto-optical modules), opto-mechanical (shutters), optical pumping elements (flash lamps and power diode modules).

The entire system must be programmed and controlled from interface programs on local computers and provide synchronization commands for the data acquisition programs and for the server to retrieve them from the global database.

2.3. Chronometer stage

The generic block diagram of a system for measuring the time between optical pulses [14] is shown in Fig. 2.3, respectively:

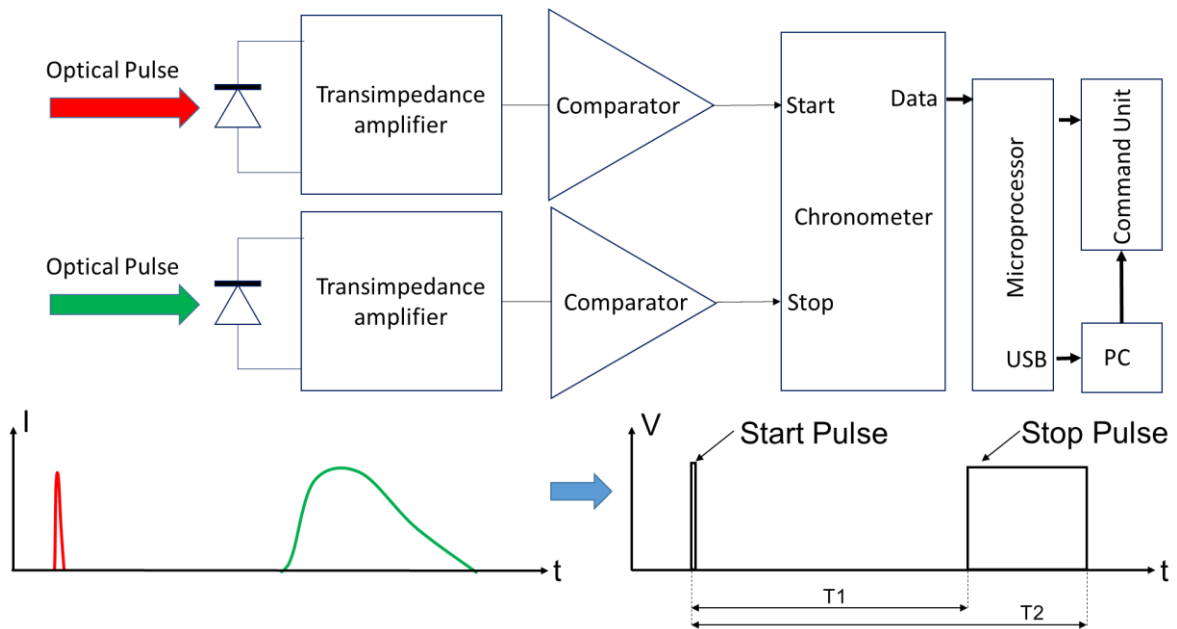


Fig.2.3. Block diagram for measuring the time between optical pulses

The scheme involves the use of ultra-fast photodiodes, transimpedance amplifiers [15] that convert the current generated into working voltage, the use of comparators for the formation of digital pulses and the digital stopwatch with time measurements between "Start" and "Stop" signals. This direct measurement method works correctly when the signals have similar amplitudes and the two signals are "clean" without artifacts generated by parasitic reflections or subharmonics. In the conditions in which the amplitude of the measured signals varies, measurement errors introduced by the fixed thresholds of the comparators appear, "slope error", according to fig.2.4.

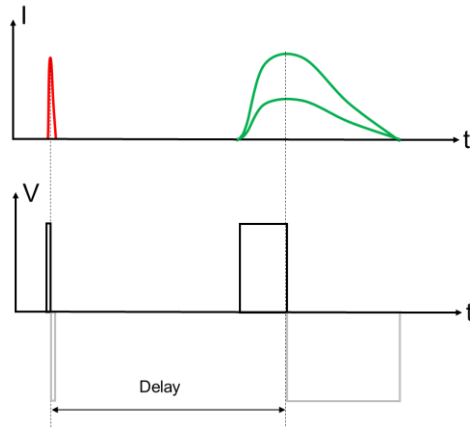


Fig.2.4. *Highlighting the temporal measurement errors given by the slope of the signals*
 The elimination of these errors can be done by measuring the derivatives of the input signals. In case the obtained signal is contaminated with multiple reflections then its derivative will generate multiple signals, fig.2.5, respectively:

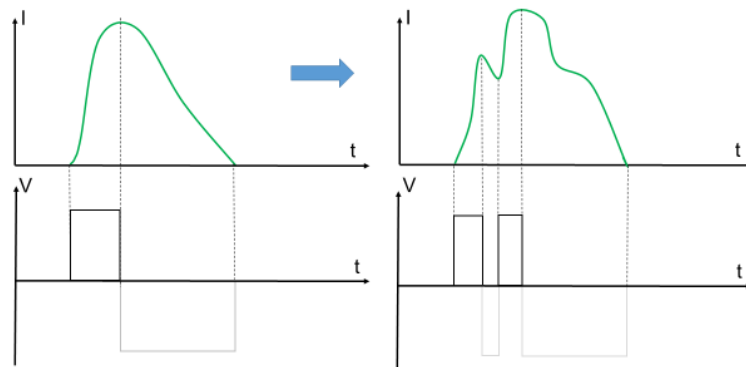


Fig.2.5. *The derivative of optical signals in ideal and real conditions*

Because an ultra-intense laser is optically noisy and the laser elements are enclosed in protective boxes with multiple reflections occurring, this measurement method cannot be applied.

In the thesis we developed an original method [16,17] which measures the delays between two signals both by the adapted derivative method and by determining the effective moments of signal generation, according to fig.2.6.

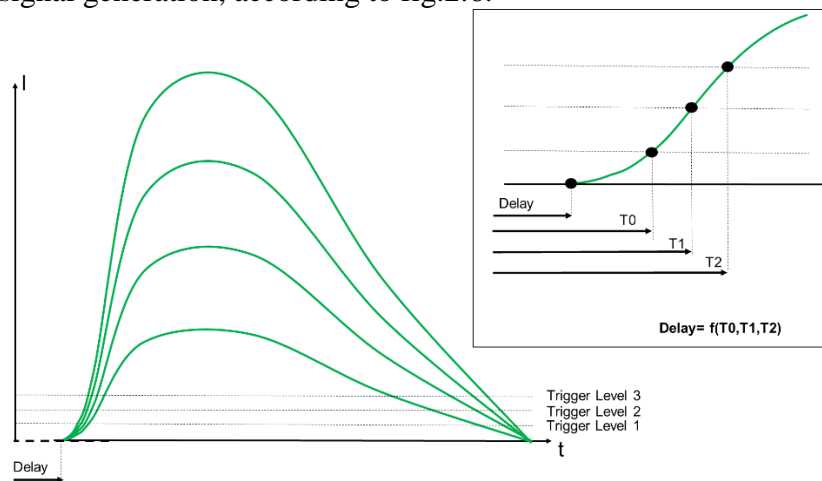


Fig.2.6. *Determination thresholds*

Basically, several time intervals corresponding to known levels of the tilting thresholds of the comparators in the system are measured, and the effective delay is calculated according to them. In order to determine the composition law, the characteristic of the system is further determined by measuring the delays without multiple reflections, the Optical Start and Stop signals having the same shape but with different amplitudes. The delay between the two optical signals is measured by the times between the maximums of the signals or having a comparison threshold by the half-sum of the switching times for both the positive front (T_0) and the negative front (T_3) according to fig. 2.7.

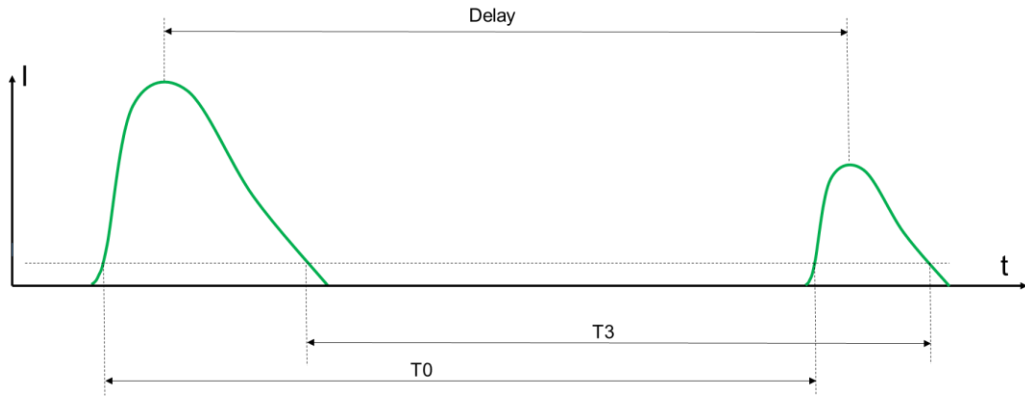


Fig.2.7. Time measurement system for undistorted signals

Basically, the delay is:

$$T = \frac{T_0 + T_3}{2} \quad (2.18)$$

Equation (2.18) is true only if $T_3 < T_0$.

And taking into account the calibrations described above the general system becomes:

$$T = \frac{T_0 + T_3}{2} \quad (2.23)$$

$$T = f(T_0, T_1, T_2) \quad (2.24)$$

In ultra-intense lasers, as the signals are periodic, delay determinations can be made between them by making time measurements alternating with a reference digital signal.

2.4. Optical path correction

In laser systems and especially in the case of ultra-intense lasers, the propagation of femtosecond pulses is critical [18]. The variations in optical path and intensity of the laser pulses that occur during propagation through the optical elements, starting from the oscillator to the target, induce either the destruction of the optical elements in the system or the loss of the fundamental characteristics of the femtosecond pulse. The problems of various optical pathways have been highlighted since the advent of femtosecond lasers, proposing solutions by using spherical and parabolic reflective optics [19] as well as active correction systems using quadrant photodiodes [20].

When propagating the laser beam through successive optical stages, the laser pulse is energetically amplified and spatially magnified by optical telescopes so as to permanently maintain the energy density below the damage thresholds of those components, usually $150 \text{ mJ} / \text{cm}^2$. Ultra-intense lasers have optical path lengths of hundreds of meters and any misalignment, especially for large diameters present in very high energy pulses, automatically leads to the destruction of optical elements.

Variations in the optical path occur in laser systems due to: the adjustment of the angle of incidence on the crystal in the case of parametric amplifiers in OPCPA lasers; variations of thermal lenses in active environments induced by cooling systems; ambient temperature variation; variation of ambient humidity; temperature variation of the optical elements in the system (mirrors); the displacements of large mirrors located in the piping when extracting air for the preparation of experiments. The compressor and the beam transport line operate at 10^{-6} mbar. All these variations of the optical path are temporarily slow and can be compensated by the additional installation in the system of some CCD video cameras and the use of motorized mounts. Thus, position monitoring is performed with near-field cameras in which the movement of the object is proportional to the movement of the spot on the CCD sensor, and far-field cameras that have an optical system with a very long focal length and on the CCD sensor is found the focal spot of the beam to be monitored and its movement is proportional to the beam angle. The block diagram of the optical path control through an ultra-intense laser proposed to eliminate the above problems is shown in Figure 2.8.

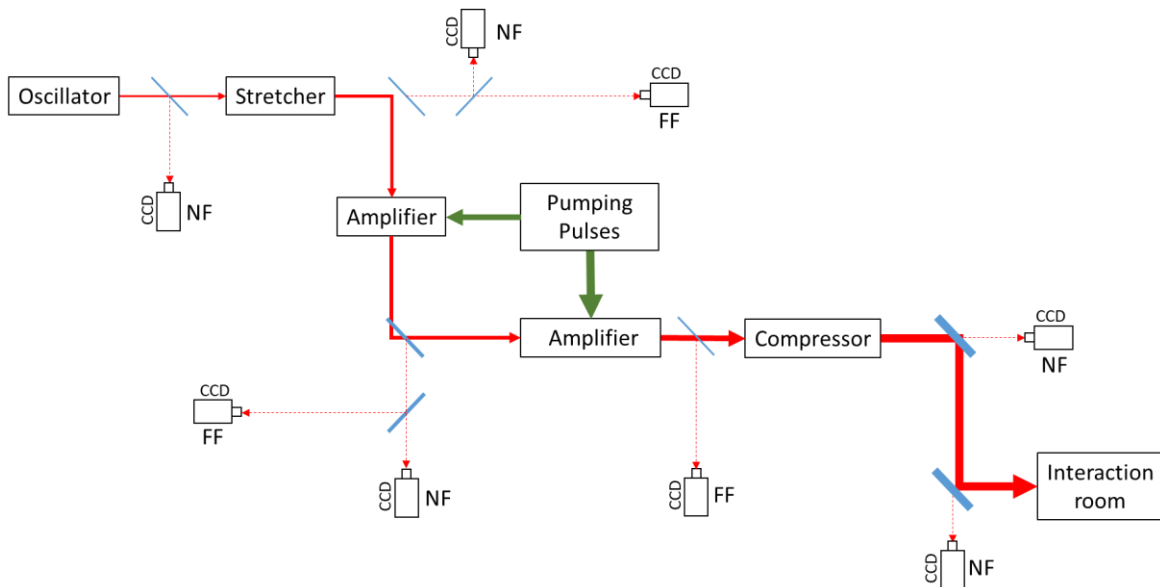


Fig.2.8. Block diagram of the control of the position of the optical beam when propagated through an ultra-intense laser

3. CETAL-PW laser system

Within INFLPR, the CETAL-PW ultra-intense laser system is installed in the CETAL infrastructure. The operation of this complex system is ensured by the following blocks:

- Laser beam conditioning - "Front-End" - fig.3.2;
- Amplifier in nominal mode - "Amplifier 2" - fig.3.3;
- PW pulse generation - "Compressor";
- Beam transport to the interaction room - "BTL";
- System for laser pulse focusing on the target.

These are presented globally in figure 3.1.

The "Front-End" laser beam conditioning stage has the role of generating laser pulses with the spectral and contrast characteristics necessary for energy amplification and compression. Depending on the characteristics of the optical elements involved, the component stages operate at various frequencies, namely 80 MHz, 1 kHz, 10 Hz and 0.1 Hz.

Amplifier 2 is a multipass laser amplifier having four passages of useful laser pulse through the active medium and energetically amplifies the laser pulse up to 30 J.

The wavefront of the amplified laser pulse is corrected by a deformable mirror, is magnified to a diameter of 160 mm, and is temporarily recompressed in the optical "compressor" to regain its duration of 25 fs and is transmitted by vacuum through the transport system "BTL", composed of dielectric mirrors M1 - M4, fig.3.5, in the interaction chamber where it is focused on the target by a off- axis parabolic mirror. The compressor and the transport system operate under vacuum at pressures of 10^{-7} - 10^{-6} mbar.

Beam monitoring is performed by video cameras placed behind the M2 and M4 mirrors, visualizing the residual transmission through the respective mirrors.

The laser controls as well as the necessary synchronizations are performed with two dedicated ISEO [25] devices developed by the manufacturer and serialized. They provide the multiplication stage functions previously analyzed in this paper and the delay control functions for each output, according to the block diagram in Figure 3.2.

The CETAL-PW laser system is a complex system that continuously provides in the interaction room a laser pulse of intensity of 1 PW. From the point of view of the command and control system, the CETAL-PW system presents the necessary synchronization blocks but which works only continuously for the two intensities of 1 PW and a working frequency of 0.1 Hz and 45 TW with a frequency of 10 Hz.

From the point of view of time control, the system does not show any monitoring, thus appearing during normal, long-term operation, time deviations (drifts) between the pumping pulses and the useful laser pulses generated by the optical path differences. From the point of view of spatial control, the system ensures insufficient control, especially in the critical area of the transport line (BTL) of the compressed laser pulse in the interaction chamber with only two control elements for 4 mirrors.

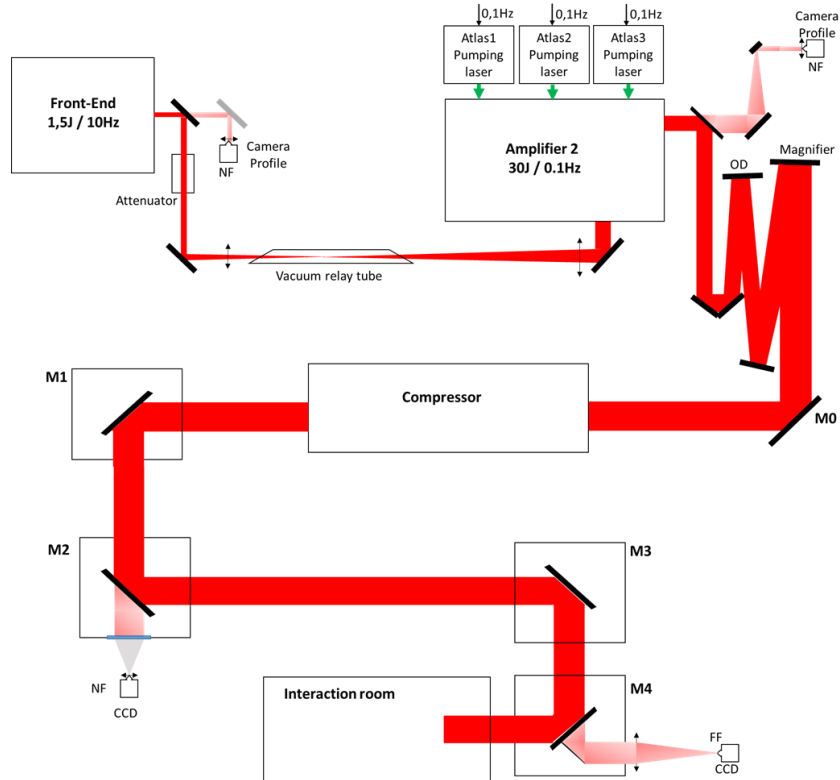


Fig.3.1. Block diagram of CETAL-PW laser system

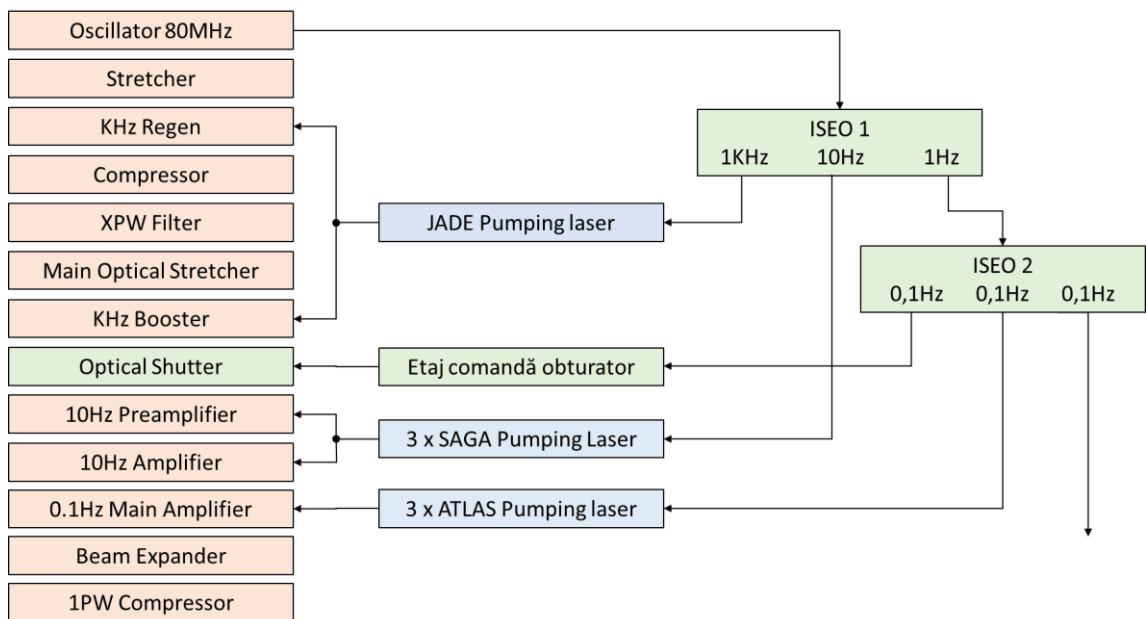


Fig.3.2. Block diagram of command system of CETAL-PW laser

4. Implementation of the adopted solutions

4.1. Introduction

The presentation of command and control solutions for ultra-intense lasers systems, made in Chapter 2, highlighted the need to implement functional blocks that must contain:

- The synchronization stage that controls the pumping lasers, ensures the selection of laser pulses through electro-optical and opto-mechanical modulators;
- The stage for measuring the time intervals between the useful laser pulse and the pump pulse (s) for maximum amplification;
- The control and correction system of the optical path by laser and by the transport system of the beam to the interception chamber.

Implementation of the solutions and their testing was performed on the CETAL-PW laser, laser presented in chapter 3.

4.2. Synchronization system – SINCROLASER

The CETAL-PW laser system has only two distinct operating modes, a peak power of 45 TW with a working frequency of 10 Hz and a power regime of 1 PW with a working frequency of 0.1 Hz. These configurations do not allow its use in pulse-to-pulse or burst mode, nor to operate at other frequencies, namely 10 Hz, 0.1 Hz, 0.05 Hz, 0.033 Hz, etc. depending on the experiment performed.

According to the operation described in the previous chapter, the commands are given by two ISEO signal generators (manufactured by Thales Laser [25]) controlled by the signal generated by the oscillator (80 MHz) and each showing a fixed synchronous clock multiplication that becomes the new synchronization signal for the remaining 20 TTL outputs with programmable frequency and phase delay versus it. All pumping lasers operate permanently at the preset frequency for thermal lens control in active environments. Pulse frequency multiplications are performed at very small beam energies and diameters with optoelectric cells (pockels cell) that ensure the selection of the working pulse by manipulating the optical polarization of both the primary series generated by the 80 MHz oscillator and the series 1 kHz secondary of the laser pulse conditioning floor. Thus before the amplification stages the pulse frequency is 10 Hz. Additional pulse selection for operation at 0.1 Hz is performed by a Uniblitz opto-mechanical shutter.

From the factory, for operation at 10 Hz, the Uniblitz shutter is permanently opened by operating the front switches and for operation at 0.1 Hz is set to "remote" and the control is

generated from ISEO2. The manipulation of laser pulses in other regimes than the initial ones can be done by additionally ordering this opto-mechanical shutter.

In addition to the controls required for pumping lasers and optical shutters, the synchronization stage must ensure the existence of physical synchronization thoroughfares (TTL) for all stages of global laser monitoring and experiment (video cameras, spectrometers, energy meters, powermeters, etc.) and also synchronization commands for the computer programs that control this equipment and for transferring data from it after the laser pulse into a database. In figure 4.1, PC1, PC2, PC3, PC4 are the initial control computers in the system (control of pumping lasers, auxiliary equipment, etc.) installed by the manufacturer and are critical elements being completely isolated from external networks to avoid illegal access. The PC Diagnostics 1, PC Diagnosis 2, and PC Diagnosis 3 auxiliary computers installed are system control computers that take data from monitoring equipment. They are wired to an INTRANET network with a database server that retrieves information from them. The Sincrolaser must control these computers to acquire the data on a pulse and the database server has to retrieve this data for permanent storage.

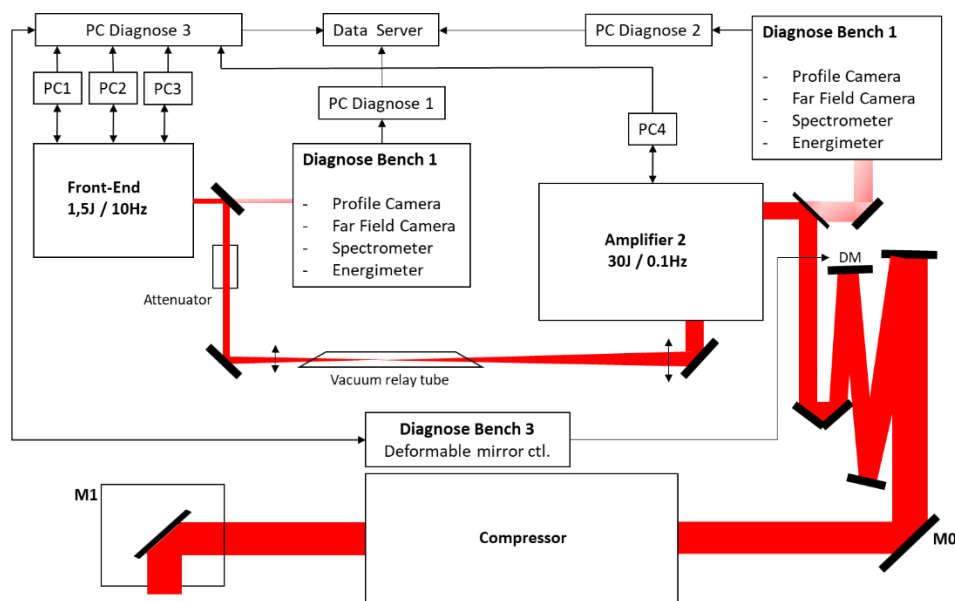


Fig.4.1. CETAL-PW laser control wiring diagram

The command of the data acquisition by the database server is ensured by the synchronous equipment by a dedicated machine that writes directly to the base a specific save indicator (flag) as well as the operating parameters.

The direct implementation of the specifications described in is shown in Figure 4.2, as follows:

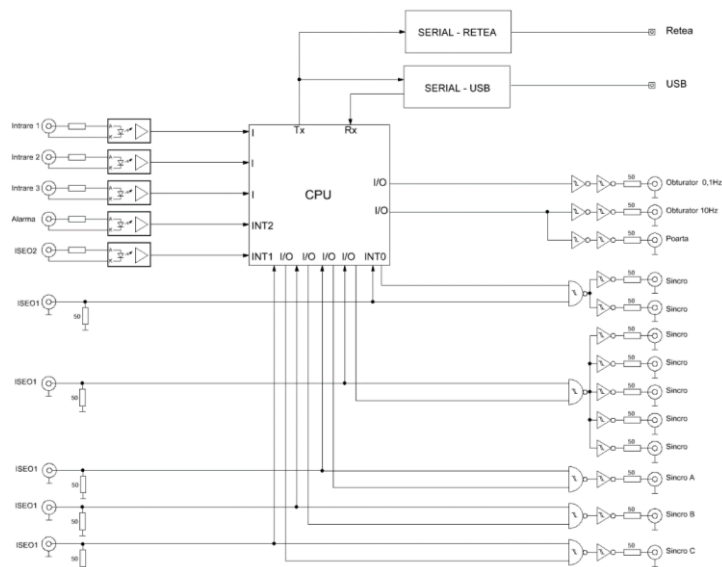


Fig.4.2. Block diagram of the synchronization equipment

Obtaining a jitter-free system involves the use of integrated circuits with Trigger Schmitt hardware inputs with tipping thresholds without variations in temperature or supply voltage which involves the use of ACT integrated circuit families [26] [27]. 50 Ω output impedances involve typical output current capability of 50 mA and with short circuit current limitation. The necessary galvanic separations are provided with ACPL-061 digital optocouplers that ensure a 10 MHz transmission, respectively 10ns switching times and TTL compatible outputs [28]. The input resistors are chosen according to the control signals so that the switching current is 5 mA.

The whole system is controlled by a processor that has the role of selection and synchronization of pulses from ISEO with the chosen working mode, communication with the computer and control of the shutters in the system. Because delay and synchronization times are generated externally (from ISEO blocks), processor decision times are not critical. A usual ATMEGA8A processor [29] controlled with a quartz crystal of 14.7456 MHz was chosen. This value was chosen to ensure a serial communication, via the USB bus, without temporal communication errors in the asynchronous transmission mode [20]. The communication is provided by the serial-USB converter obtained with FT232R [30] which provides all the necessary functions and the electronic diagram is shown in fig.4.10.

Figure 4.3 contains a general diagram of the motherboard of the Sincrolaser equipment.

The Serial-Network Converter was made using the USB-controlled Raspberry PI microcomputer [31] only on the Tx transmission control via an additional FTDI FT232R [30] circuit. The database communication software was developed in Python 3.0.

The implemented scheme is shown in figure 4.4.

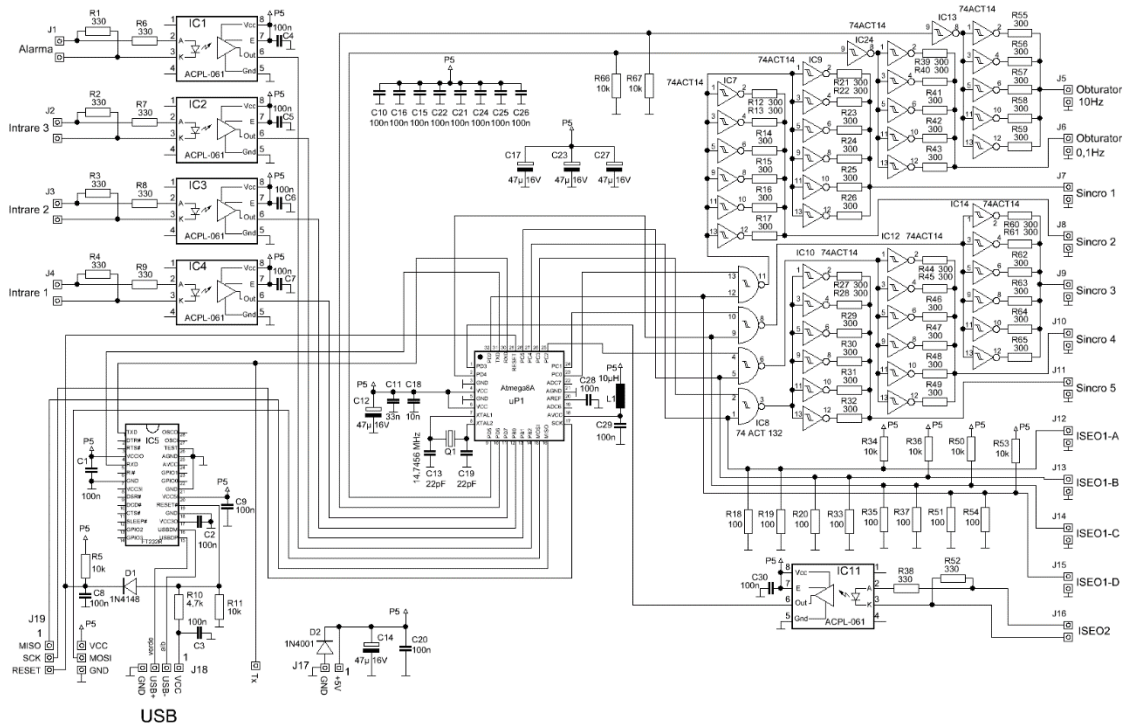


Fig.4.3. Electronic scheme implemented

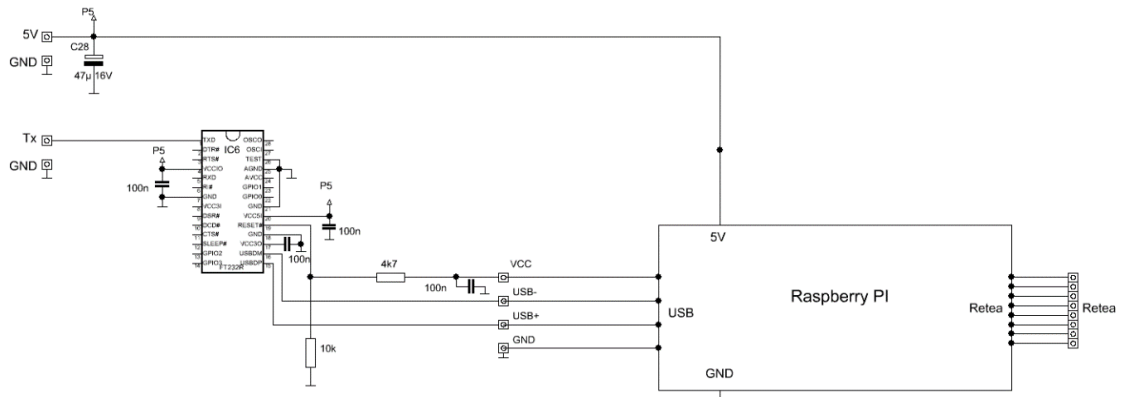


Fig.4.4. Electronic schematic of the Tx - Network Server converter

The control program was made in LABVIEW [32] for reasons of compatibility with the rest of the laser control programs and the graphical interface is shown in figure 4.5:

The software in the microcontroller is made in assembly language and ensures: serial communication with the control computer via a USB interface and the physical control of the CETAL-PW laser depending on the external commands. All outputs are synchronous with the laser clock. The flowchart of the communication program on the control interface computer is defined simplified in Figure 4.6.

The actual controls of the 10 Hz and PW frequency shutters (0.1 Hz or submultiples) and the blocking of the laser controls depending on the working modes (pulse by pulse or burst) are performed synchronously on the Int0 and Int1 interrupts of the processor.



Fig.4.5. Stage control program interface

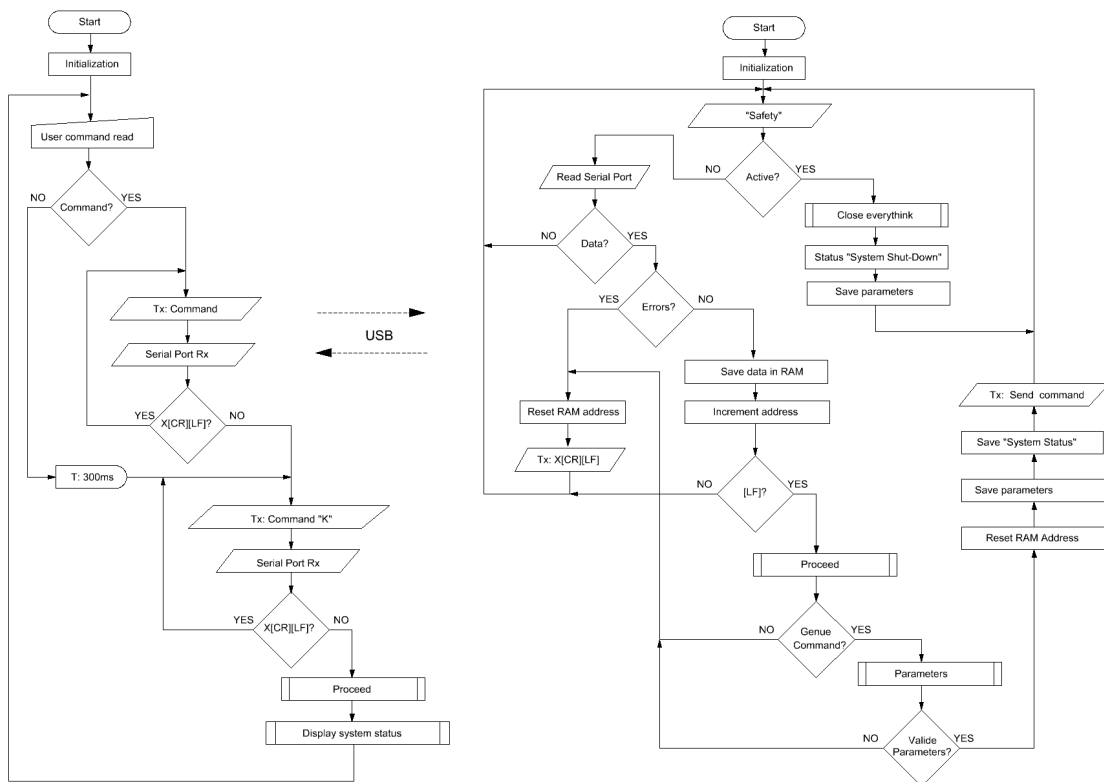


Fig.4.6. Organization charts of communication and command programs

The system response that completely defines the status is also read by the Raspberry PI microcomputer via the USB interface. It writes through a Python script in a database the system status and the time until the next pull, thus ensuring the synchronization of the programs (software) of the data saving computers.

4.3. Temporal monitoring system of optical pulses from ultra-intense lasers

For the operation of ultra-intense lasers, the synchronization between the useful pulse and the pumping pulse(s) is critical, any desynchronization generates the elimination of the optical pulse amplification or its superficial amplification.

The CETAL-PW laser system shows the time diagram of the laser pulses in the main optical amplifier shown in fig. 4.22 from a functional point of view.

Their synchronization is defined by the architecture of the main amplifier, specified as “Amplifier 2” in figure 4.4 and with the optical paths described in figure 3.3. This is a 4-pass multipass optical amplifier. The optical path made by the useful laser between two passes is 6 m which corresponds to a time interval of 20 ns and the laser pulse has a time width of 800 ps at half height. Atlas pumping lasers generate pulses with a duration of 15 ns at half height and provide two phase shifted pulses with 55 ns between them. The time diagram of the pulses through the crystal is defined in figure 4.7.

Thus the monitoring stage must be able to measure delays between signals in the range 1 ns - 1 μ s with a resolution of 1/10, respectively 50 ps -100 ps.

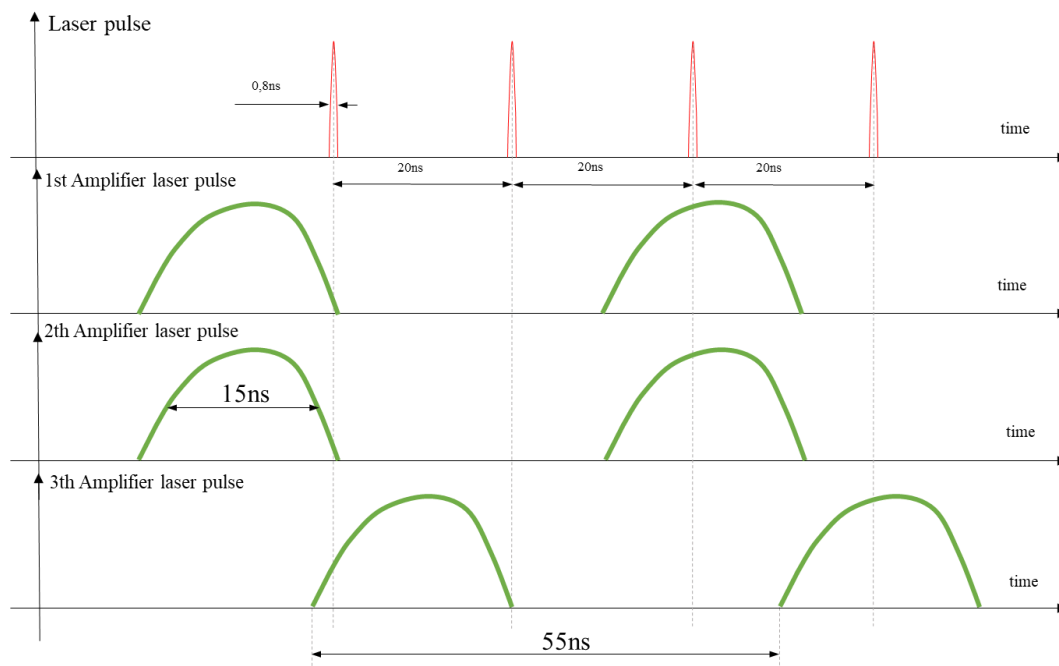


Fig.4.7. Time diagram of optical pulses in the multipass amplifier

According to the specifications it is necessary to use an integrated timer circuit with a measurement resolution below 50 ps and capable of measuring time intervals of 1 μ s. During the implementation we chose the integrated circuit timer type MSC Vertriebs GMBH TDC 502 [36] and the main features are described in table 1:

Table 4.1. Characteristics of MSC Vertriebs GMBH TDC 502 circuit

Resolution	45ps
Measurement modes	range I: Ops – 10μs ; range II: 180ns – 210ms
Channels	2 channels with a common Start, rising or falling edges individually programmable
Multihit capability	up to 10-fold multihit capability and up to 10 measurements within a burst
Calibration Clock	External crystal clock required, 500 kHz – 20 MHz
Calibration measurement	Automatically after time measurement or stand-alone
Time measurement	Every hit to start and every hit to each other hit
Output data resolution	24 bit unsigned integer number

Chapter 2 described the innovative method of measuring these phase shifts by simultaneously determining several time intervals, for various physical thresholds and obtaining the actual delay by calculations relative to the intervals obtained.

Basically, four time intervals must be measured simultaneously in parallel, three for the rising front and one for the decreasing front. The usual stopwatch circuits (including the chosen circuit) allow one or two stop inputs, respectively one for ascending fronts and one for descending fronts and additionally allow cascade measurements.

The solution is to serialize the parallel pulses generated by the comparison thresholds [16], [17], according to Figure 4.8.

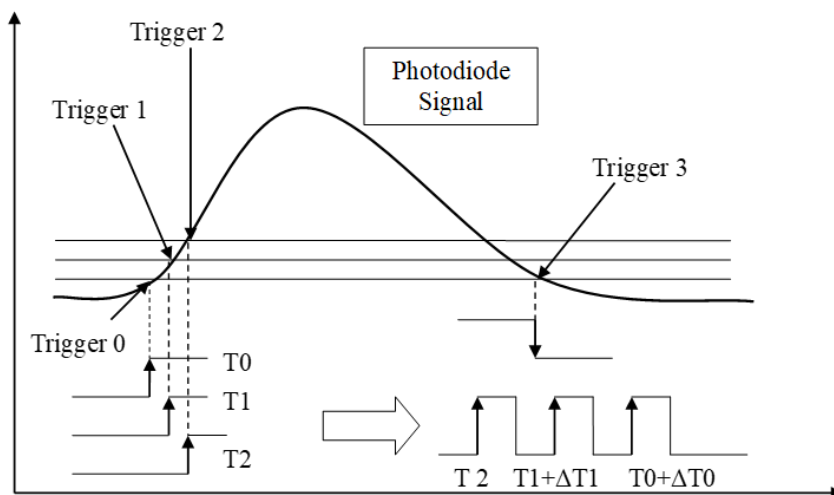


Fig.4.8. Block diagram of delay transformation by serialization, [16], [17]

Thresholds 0,1 and 2 represent the switching voltages (active on the positive front) of the comparators that monitor the output signal corresponding to the optical signal and ΔT_1 and

ΔT_2 are the delays introduced in the system for the safe detection of the pulses. The threshold signal 3 represents the output of the threshold comparator 0 but activated on the negative front. Practically from the difference of the delays defined by the thresholds 3 and 0 the duration of the optical pulse is defined. The chosen timer circuit requires that the additional delays ΔT_1 and ΔT_2 be at least 25 ns, in order to perform the measurements correctly and the minimum duration of the Start and Stop pulses of 14 ns. The proposed diagram of temporal serialization of the pulses is specified in figure 4.25 and the physical implementation in figure 4.9. The required delays were obtained with transfer gates with hysteresis 74AHC14 [37] and 74AHC132 [38] which have the typical transfer delay of 11 ns and a maximum of 21 ns, known. By adding 2 k Ω resistors in conjunction with the parasitic input capacities of 50 ps, delays of 50 ns - 80 ns can be obtained. The delays introduced are not critical because in the measurement described in Chapter 2 they are eliminated by successive measurements of the pulses involved. They are chosen for tens of nanoseconds.

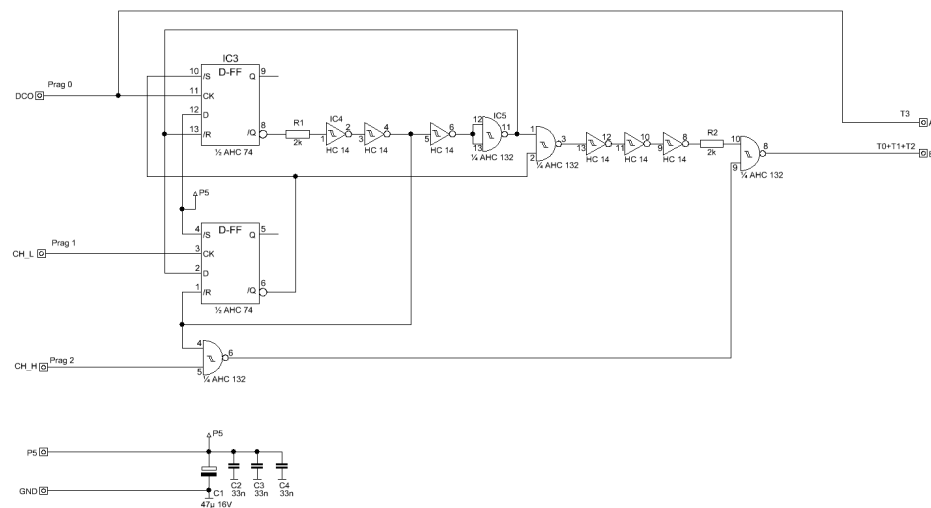


Fig.4.9. Electronic time serialization scheme implemented

The reception of the system we chose to be done with the ELECTRO-OPTIC DEVICE ERX-6 board [39] which generates two signals, one digital and one analog corresponding to the optical input of the embedded silicon photodiode. This is a compact board powered directly at 5 V and provides a transimpedance of 1000 k Ω .

The central unit controls all electronic subsystems so a microcontroller must be chosen to include the necessary interfaces (CAN, Serial, parallel ports), analog-to-digital converters, counters, non-volatile and volatile memory and interrupt operation. To achieve these goals, the ATMEL AT90CAN32 microprocessor [40] was chosen, for maximum flexibility. To ensure error-free USB communication the system clock is chosen multiple of 2 respectively $Q = 14.7456$ MHz. The implemented block diagram is shown in figure 4.10.

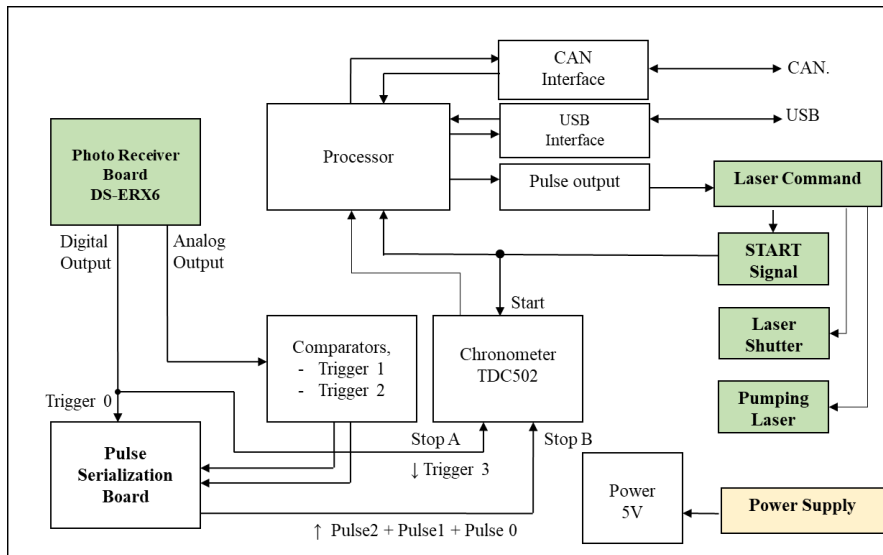


Fig.4.10. Block diagram for time monitoring equipment

Basically, the time period between the “START” signals, a digital signal generated from the “Sincrolaser” equipment developed in the thesis (Chapter 4.2) and the optical pulse “STOP” from main laser amplifier, according to Figure 4.11, are determined.

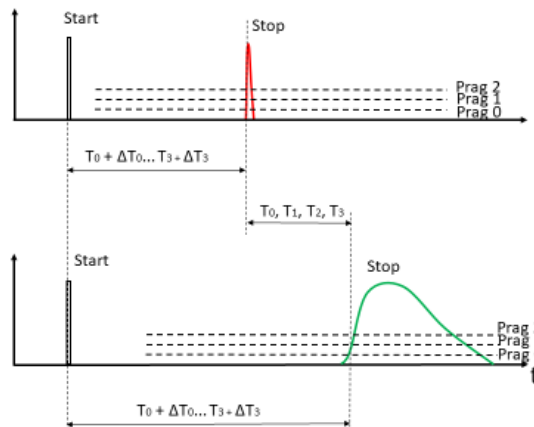


Fig. 4.11. Implemented timing diagram

The signals generated by the ELECTRO-OPTIC DEVICE ERX-6 optical reception stage [39] are a digital one - DCO- with a minimum threshold automatically set at the detection limit and which in the stage becomes threshold 0 for the rising edge and threshold 3 for the decreasing edge and an analog signal proportional to illumination - ASO. Since this signal is proportional to both the ambient lighting and the signal given by the laser pulse, the detection thresholds - threshold 1 and threshold 2 will have a fixed voltage component overlapped with a voltage proportional to the ambient lighting. The implemented electronic scheme is shown in figure 4.12.

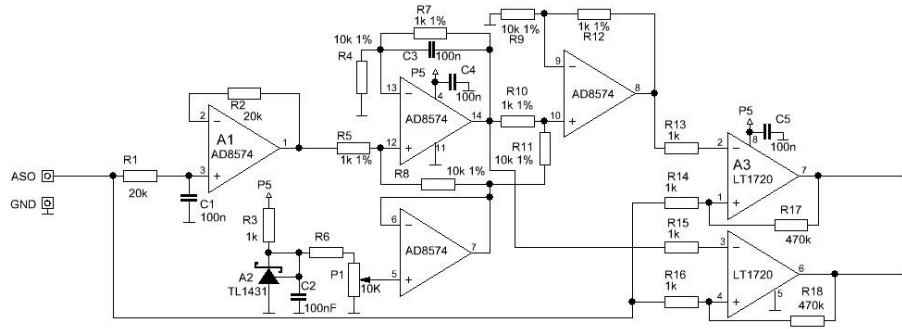


Fig.4.12. Electronic comparison scheme for time thresholds

Comparison threshold voltages are:

$$V_{Prag1} = V_{ASO} + V_{P1}/10 \tag{4.5}$$

$$V_{Prag2} = V_{Prag1} + V_{P1}/10 = V_{ASO} + V_{P1}/5 \tag{4.6}$$

The external communications of the microsystem are made through the FT232R converters for the USB bus and the MCP2551 for the CAN bus. The TDC502 timer circuit interfaces with the microprocessor through a one-byte data bus (DATA0-7), address bus (ADR0-3) and related activation signals (read, write, select, etc.). In addition, it has a status output - "ready to start" as well as an output for external interruption - "measurement completed". The stopwatch circuit can operate in several operating modes such as 1 channel (A or B) with cascade measurements of up to 10 pulses or 2 channels simultaneously with cascade measurements for 4 pulses etc.

The overall scheme of the equipment is shown in figure 4.13.

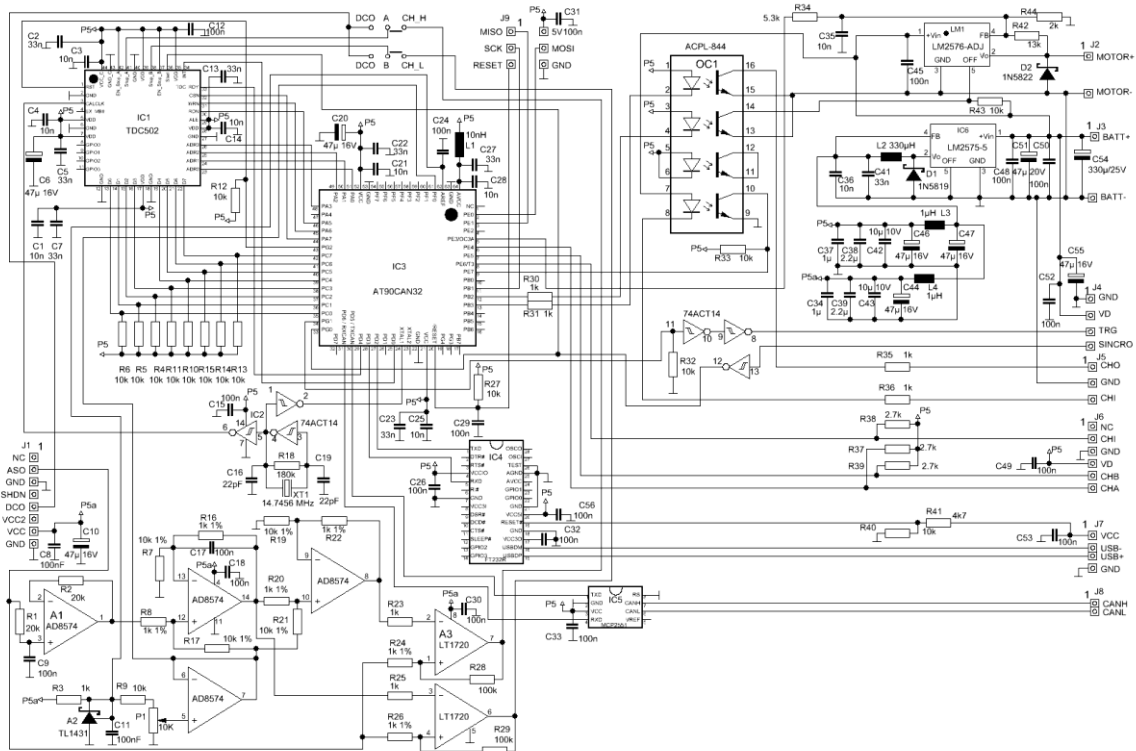


Fig.4.13. Complete electrical diagram of the Chronometer stage

The microsystem program was written in assembly language and was structured on priority levels: the serial communication loop ensures communication with the computer, the interpretation of commands and the setting and reporting of the system status; "10 Hz" loop, externally controlled on the INT0 interrupt, corresponding to the measurement of the useful laser pulse ("seed") compared to the start signal generated by the Synchronolaser; "0,1 Hz" loop controlling the laser in PW mode (0,1 Hz or submultiples), externally controlled on the INT1 interrupt, corresponding to the measurement of the pumping laser pulses compared to the starting signal generated by the Sincrolaser equipment. The control of the equipment is performed through a serial communication via a USB interface, using its own terminal program. From the moment of the start command, the phase shift between the electrical signal generated by the Sincrolaser synchronization stage and the laser pulse is measured every 100ms (interruption of INT0). The interrupt INT1 generates the measurement of the delay between the electrical signal generated by the Sincrolaser synchronization stage and the pumping laser pulse. The useful laser signal is blocked by activating the opto-mechanical switch Sh1. Figures 4.14 and 4.15 show the flowcharts of the described program.

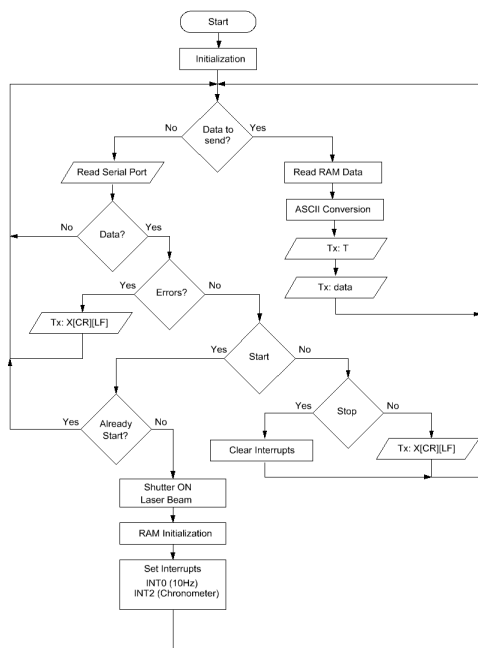


Fig.4.14. Flowchart of the microprocessor program for the main loop

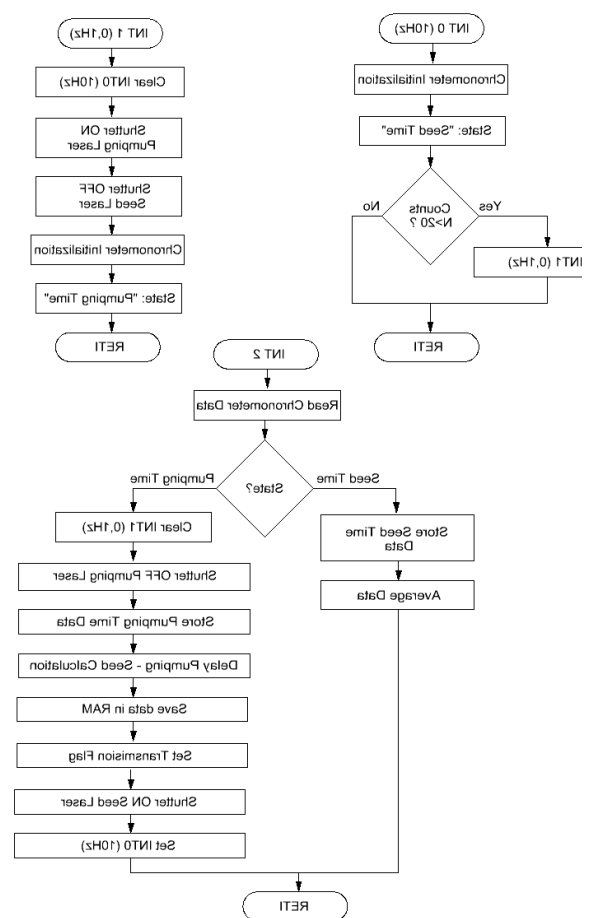


Fig.4.15. Flowchart of the microprocessor program for the interrupts

Statistics were performed on a series of 20 time measurements between the laser pulse and the pulses of the pumping lasers and displayed graphically in Figures 4.16, 4.18 and 4.20. The equation for determining the temporal phase shift between the useful laser pulse and the pumping pulses is shown in Figures.4.17, 4.19 and 4.21 corresponding to pumps 1, 2 and 3. On the abscissa are the partial phase shifts and on the ordinate the thresholds. The times determined for the phase shift between the useful laser pulse and the pumping pulse 1 are:

- mean: $T = 20.278$ ns; minimum: $T_{min} = 19.946$ ns; maximum: $T_{max} = 20,508$ ns
- The maximum error is: $\varepsilon = \pm 1.38\%$; the standard deviation is: $\sigma = 0.68\%$
- Determination resolution: 45 ps

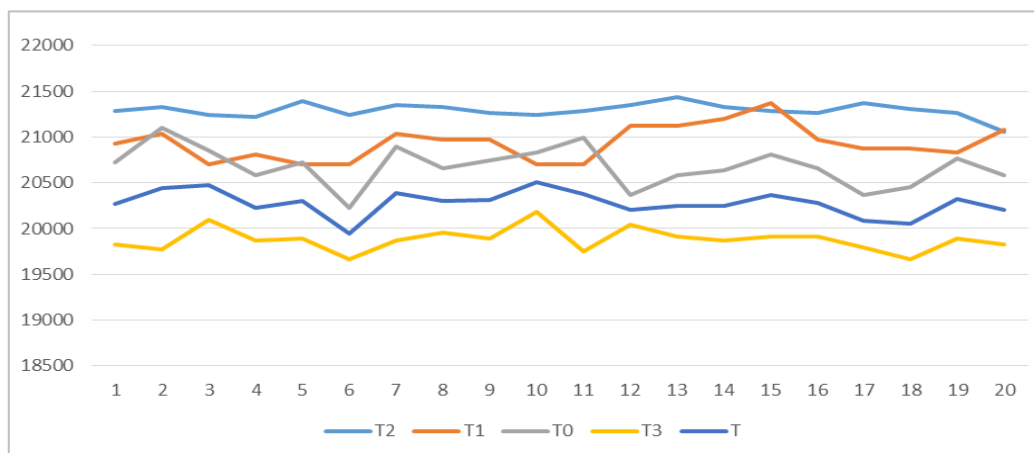


Fig.4.16. Time measurements for phase shift between useful pulse and pumping 1

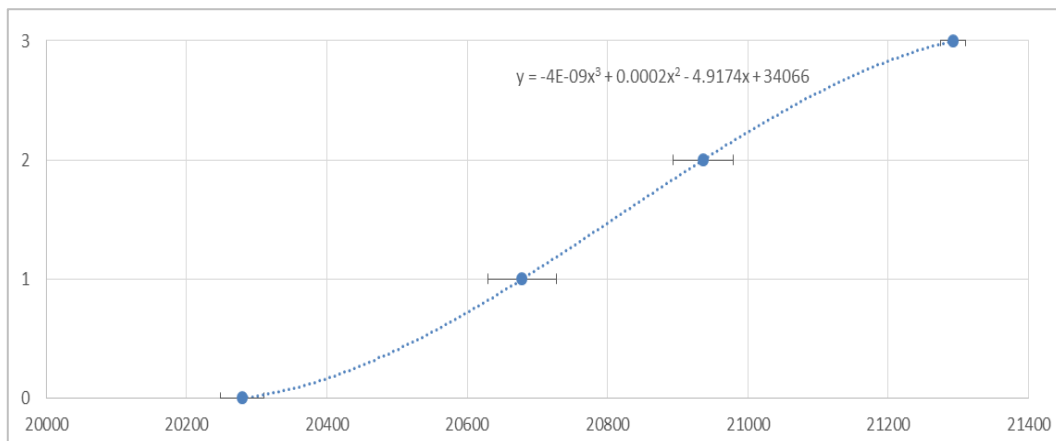


Fig.4.17. The law of calculating the real time interval between the useful pulse and the pumping 1

The times determined for the phase shift between the useful laser pulse and the pumping pulse 2 are:

- average: $T = 20,320$ ns; minimum: $T_{min} = - 20,159$ ns; maximum: $T_{max} = 20,531$ ns
- The maximum error is: $\varepsilon = \pm 1\%$; the standard deviation is: $\sigma = 0.5\%$
- Determination resolution: 45 ps

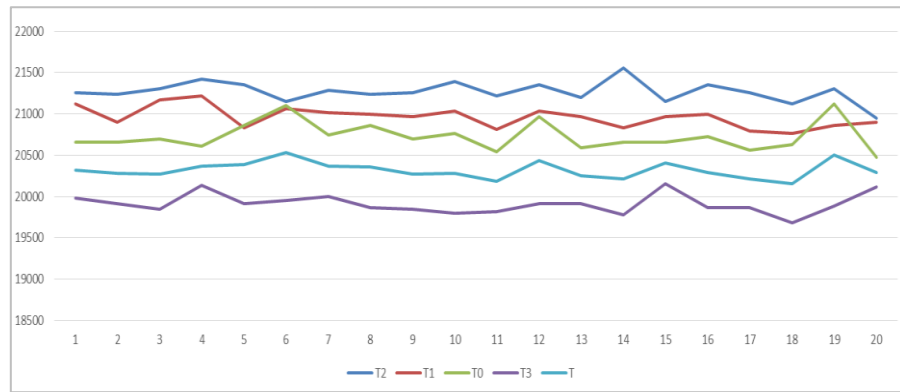


Fig.4.18. Time measurements for the phase shift between the useful pulse and the pumping 2

The equation for determining the phase shift between the useful laser pulse and the pumping pulse is shown in Fig.4.38.

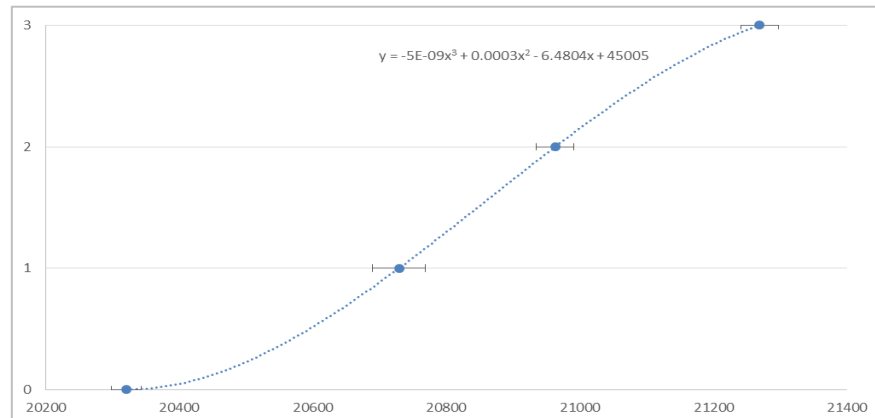


Fig.4.19. The law of calculating the real time interval between the useful pulse and the pumping 2

The times determined for the phase shift between the useful laser pulse and the pump pulse 3 are:

- average: $T = 4,409$ ns; minimum: $T_{min} = 4,203$ ns; maximum: $T_{max} = 4,603$ ns
- The maximum error is: $\varepsilon = \pm 4.54\%$; the standard deviation is: $\sigma = 2.31\%$
- Determination resolution: 45 ps

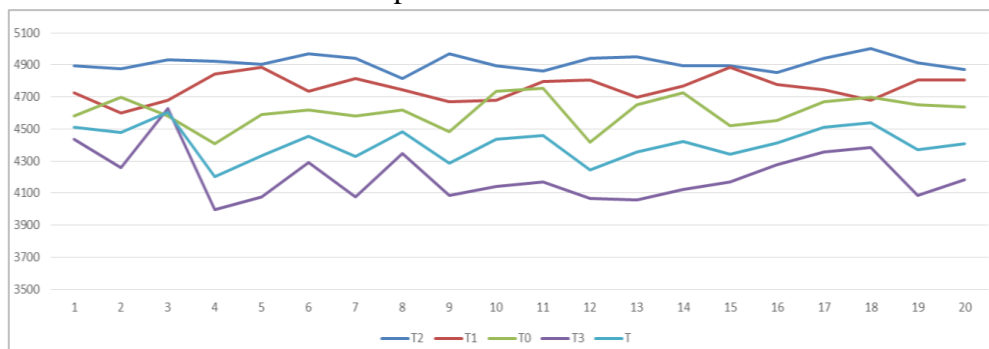


Fig.4.20. Time measurements for the phase shift between the useful pulse and the pumping 3

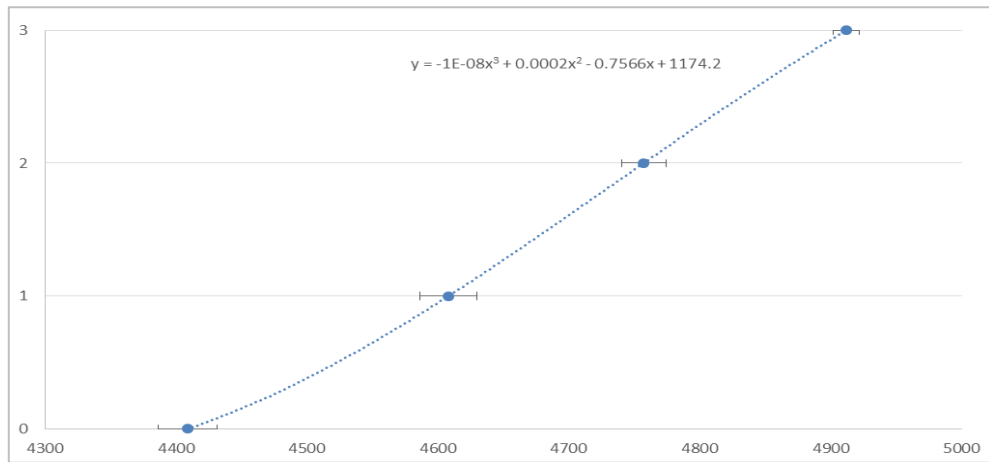


Fig.4.21. The law of calculating the real time interval between the useful pulse and the pumping 3

4.4. Beam position control system for CETAL PW laser

OPCPA and CPA ultra-intense lasers systems have total optical path lengths of hundreds of meters, for example the CETAL-PW laser shows an optical path through all laser amplifiers to the interaction chamber around 150 m. Incidence angle settings for amplification from OPCPA lasers as well as small variations due to thermal expansion of mounts or small misalignments of optical components translate for these optical path lengths to significant variations in position and trajectory of the laser beam as it passes through the amplifier blocks and in the transport system connecting the compressor of the interaction chamber. In this area the laser pulse has the maximum intensity and diameter which requires its propagation through high vacuum and variations in position and inclination lead to parasitic laser beams generated by the intersection of the laser pulse with the piping walls of the transport system which in turn lead to focal spots on the surfaces of the mirrors in the system, which involves their destruction [41].

At the exit of the laser conditioning stage ("Front-End") the beam has a diameter of 12 mm, at the exit of Amplifier 2 its diameter is 60 mm, and at the entrance to the compressor it becomes 160 mm. From this point it is delivered to the interaction chamber, under vacuum, through a pipe with an inner diameter of 240 mm. The compressor of the CETAL-PW laser system as well as the subsequent stages works in vacuum, at a pressure of 10^{-6} mbar. In the stages preceding the experiments, the alignments and verifications are performed in air and its extraction leads to the modification of the positions of the large mirror mounts located in the tubing (320 x 230 mm) leading directly to the catastrophic displacement of the laser beam.

Beam position and direction monitoring is performed with Near-Field cameras being solved directly by mounting the cameras at the output of each functional optical block, according to Figure 4.22.

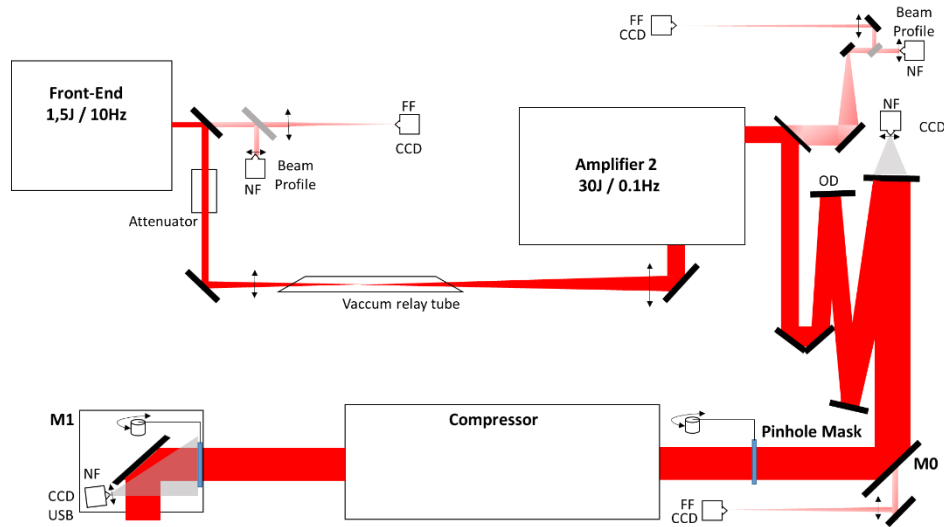


Fig.4.22. Optical scheme implemented in the CETAL PW laser for spatial control of the laser beam. This optical diagram was shown in [21], fig.3.

Given that the diameter of the laser becomes 160 mm, the direct use of near-field cameras is not feasible - the displacements of the order of millimeters cannot be highlighted. For this reason, the solution of using an optical pinhole mask has been implemented that allows only parts of the beam to pass and thus allows clear highlighting of the center of the beam and the concentricity of the beam with the central circle, respectively the ring segments in concentric circles must have the same illumination. The implementation of this mask was done by fixing it on a rotating axis at the entrance to the compressor and within the alignment being automatically inserted or removed from the attenuated laser beam.

The control of the position of the laser beam involved the use of semi-transparent screens, mounted on motorized rotating axes, located in front of the mirrors in the beam transport line and of some near-field type cameras that monitor the beam through the transparency of the screens. Additionally, these screens protect the mirrors from parasitic foci. Thus, a unique system determined by the position of the laser beam is obtained through the entire transport system. The optical scheme implemented for the transport system is shown in fig.4.23.

The necessary screens were made of Teflon plates, a material with a very high melting point, 326.85°C , a very low vacuum gasification rate and a sufficient degree of transparency (1%) for the video cameras used. STANDA goniometers type 7R150V were used to move the screens, allowing: 360° rotation, angular speed of 8 rpm, angular resolution of 2 arcmin, radial load 1.7 kg and vacuum operation. Selected used video cameras: Microsoft USB Cam3000HD, with HD resolution, autofocus and vacuum operation. For the physical construction of the systems it was not allowed to make any mechanical modification

(drilling, threading, etc.) so that localized custom solutions were used. The projects were personally carried out in SolidWorks 2012.

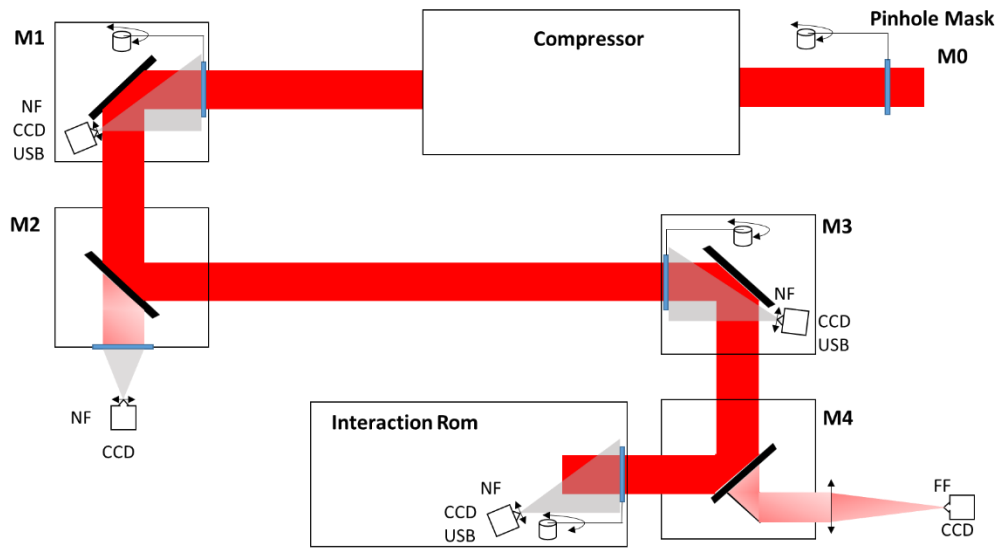


Fig.4.23. Optical scheme implemented in the CETAL PW laser for the spatial control of the laser beam through the transport line. This optical diagram has been displayed in [21]

The command and monitoring system was made by separating the control areas: the laser area that controls and monitors the pinhole's position, the Far-Field and Nier-Field laser cameras and the screen and video camera from the M1 transport mirror (Ground floor) and the transport area controls and monitors the screens and video cameras from the M2-M4 mirrors and in the interaction chamber (Basement). The block diagram of the control floors for the upper and lower beam transport line is shown in Figure 4.24. Figure 4.25 shows the alignment of the CETAL-PW beam transport line, highlighted with the images obtained by the cameras mounted in the system.

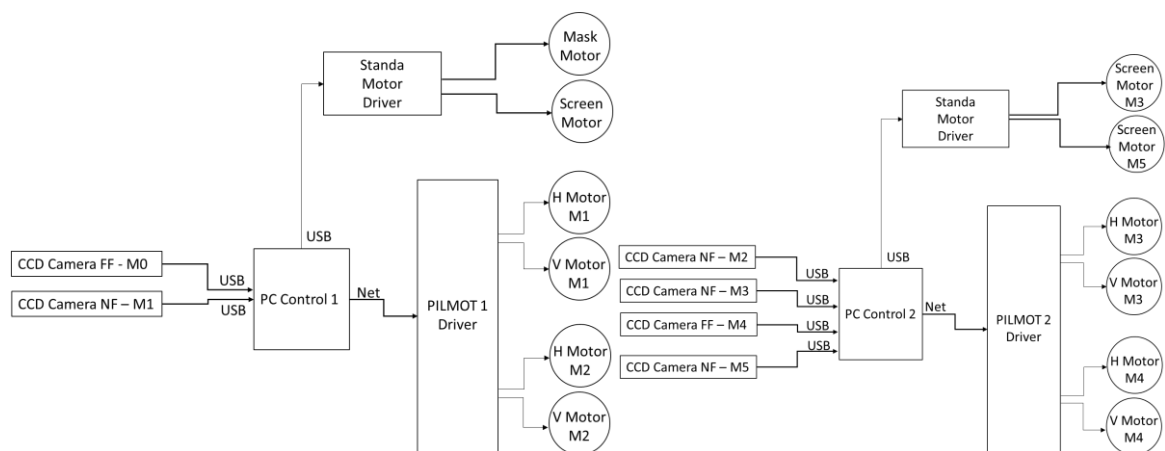


Fig.4.24. Diagram of the control stages of the spatial control of the laser beam through BTL

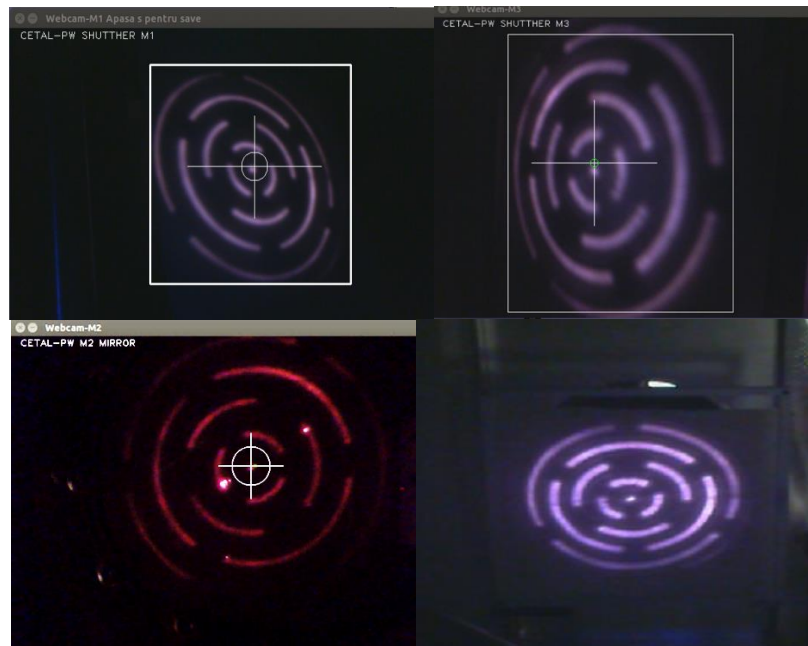


Fig.4.25. Control images for mirrors M1, M2, M3 and M4. Similar images were shown in [21] fig. 9

5. Applications of developed solutions in laser scanning

Within the doctoral school I developed an original method for measuring the time intervals between optical pulses. The immediate application is in the implementation of a laser scanner with applications in the automotive industry [16] [17], an application imposed by a research contract with Optoelectronica 2001 SA for the development of such equipment and is the continuation of a European research contract of this company, respectively “Enhanced Road Safety by integrating Egnos-Galileo data with on-board Control system - ERSEC”. Following the analyzes performed, the necessary specifications of the scanner are: scanning distance: 0.3 m ... 50 m; Scan frequency: 50 Hz; Scan opening: 180°; Resolution 1 cm and Angle increment: 0.5°. Their implementation involves the characteristics of the necessary electronic floors, respectively: Power supply from 12V car battery (11V-15V); OSRAM SPL LL90_3 laser diode (50W pulse); chronometer with a resolution of 66 ps (corresponding to a measuring resolution of 1 cm); USB or CAN communication; mechanically connected motor with deflection mirror and angular position encoder; microcomputer; synchronization with an external scanner and local power supplies (5 V etc). The optimal optical scheme determined is shown in Figures 5.1 and 5.2. The control scheme developed in determining the phase shifts in the CETAL-PW laser was used, but instead of the Synchrolaser, the system controls a DC motor and the synchronization pulses are generated by the HED5540 rotary decoder coupled to the motor shaft.

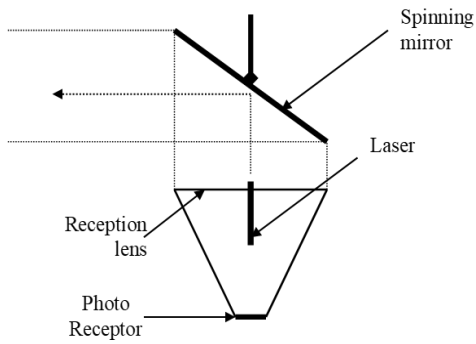


Fig.5.1. Functional diagram for laser scanning, side view

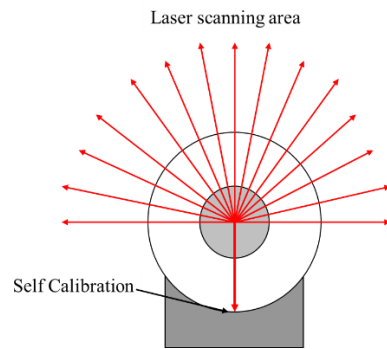


Fig.5.2. Functional diagram for laser scanning, top view

The block diagram of the system is shown in figure 5.3 and the results obtained in fig. 5.4.

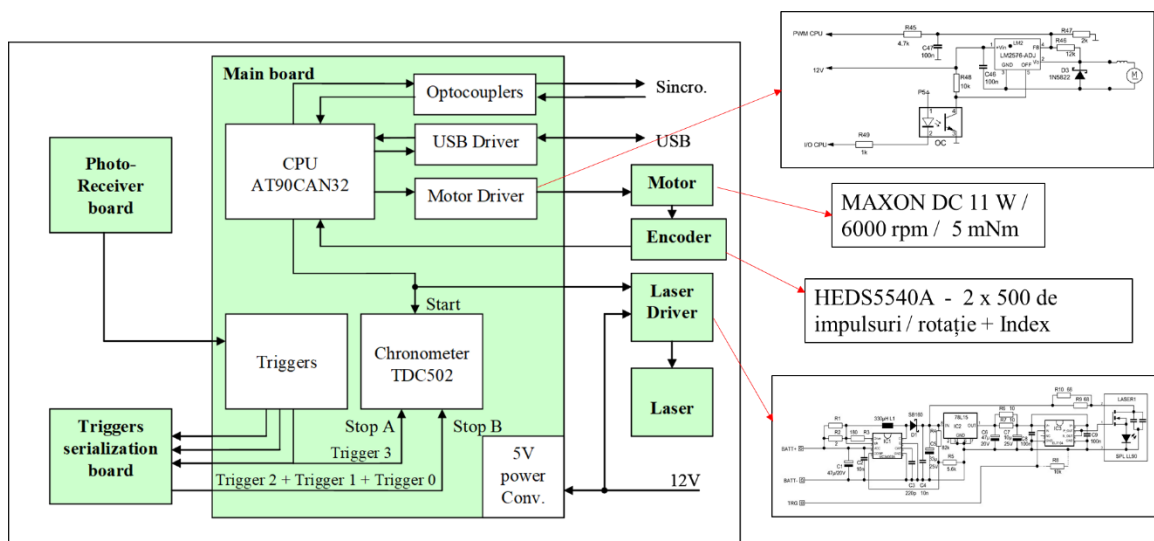


Fig.5.3. Block diagram for the laser scanner

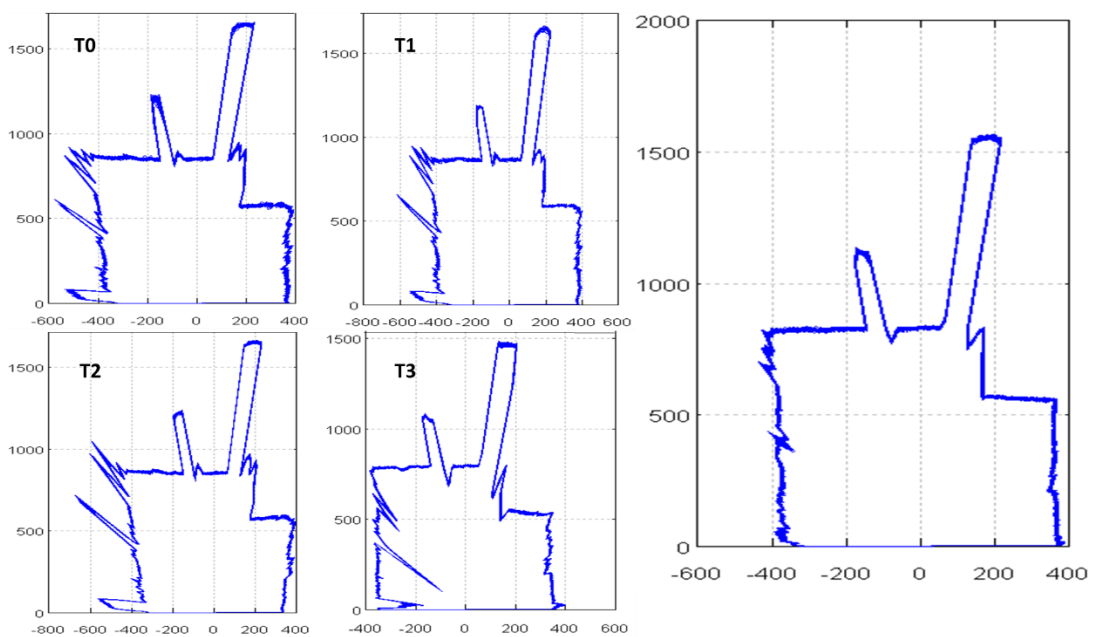


Fig.5.4. The results of scanning a room for each threshold. Results in cm.

6. Conclusions

In this doctoral thesis I developed, designed and implemented a command and control system of ultra-intense lasers and was integrated into the CETAL-PW laser.

With this, complex laser-target interaction experiments were performed using the command and control systems developed in this thesis, as follows:

- The control of the laser regarding the pulse-by-pulse and burst operation for the 45 TW regime and the 10 Hz frequency allowed the performance of experiments of temporal enlargement of the laser pulses through thin foils. The results were published in [42].
- Pulse-to-pulse laser control for the PW mode allowed complex experiments on the interaction of the laser pulse with solid targets. Basically, experiments were performed to accelerate electrons in solid targets and the pulse-to-pulse working regime was used with a working cadence of 1 pulse at 10 min. The results were published in [33] and [34].
- Laser control on burst operation in PW mode and with frequencies of 0.05 Hz allowed experiments to be performed on obtaining electrons accelerated with energies of hundreds of MeV in the gas jet.

The temporal monitoring system ensures the determination of the phase shift between the useful laser pulses and the pulses of the pumping lasers. During the implementation in the CETAL-PW laser, the specific delays were measured, in class 1 ns -20 ns.

The beam position control system implemented in the CETAL-PW laser ensures laser beam control and eliminates critical misalignments in the transmission line.

Laser scanning data obtained using the time interval measurement solution by the original method developed are published in [16] and [17].

The original contributions are:

1. I developed and implemented a new concept on temporal measurements between optical signals, which eliminates measurement errors due to amplitude differences between signals (slope errors) and errors generated by their multiple reflections.
2. I have developed a control and command equipment for ultra-intense lasers in pulse-to-pulse shooting mode, continuously and in bursts.
3. I developed an original system based on the control of the position of the laser pulses through the transparency of specific curtains for the spatial control of the position of the laser beam through the transport system. This technique protects the vulnerable mirrors during the adjustment stages preceding the PW class laser pulses.
4. The concepts developed were validated in a laser scanning equipment.

The research results are directly applicable to high power class lasers such as the 2 x 10 PW ELI-NP and the new 100 PW laser concepts.

Bibliography

- [1] D. Stricklan, G. Mourou, *Compression of amplified chirped optical pulses – Optics Communications*, Vol. 56/3, Pag. 219-221, 1985;
- [2] “The White Book of ELI Nuclear Physics Bucharest-Magurele, Romania”, <https://www.eli-np.ro/documents/ELI-NP-WhiteBook.pdf>
- [3] Rongtao Su, Pu Zhou, Xiaolin Wang, Yanxing Ma, Xiaojun Xu, “Active coherent beamcombination of two high-power single-frequency nanosecond fiber amplifiers” – *Optics Letters*, Vol. 37, No. 4, 2012;
- [4] Arno Klenke, Enrico Seise, Jens Limpert, Andreas Tunnermann, “Basic considerations oncoherent combining of ultrashort laser pulses” – *Optics Express*, Vol. 19, No.25, 2011;
- [5] J A Fülöp, Zs Major, A Henig, S Kruber, R Weingartner, T Clausnitzer, E-B Kley, A Tünnermann, V Pervak, A Apolonski, J Osterhoff, R Hörlein, F Krausz and S Karsch, “Short-pulse optical parametric chirped-pulse amplification for the generation of high-power few-cycle pulses” *New Journal of Physics*, Volume 9, December 2007
- [6] Răzvan Dabu, „Lumina Extremă - Lasere de mare putere”, Editura Academiei Române, ISBN 978-973-27-2561-0, 2015;
- [7] D. E. Spence, P. N. Kean, and W. Sibbett, “60-fs Pulse Generation from a Self-Mode-Locked Ti:Sapphire Laser” – *Optics. Letters*. Vol. 16, Pag. 42, 1991;
- [8] Thales Laser, *1PW Cetal laser User Manual*, 62538166AA-108;
- [9] W. Koechner, *Solid State Laser Engineering, Capitolul 1*, Springer Verlag, Berlin, Heidelberg, 2006
- [10] Paul Schiopu, *Optoelectronics*, Ed. MATRIXROM,2009, ISBN 978-973-755-443-7
- [11] Uniblitz VCM-D1 User Manual, <https://www.uniblitz.com/products/vcm-d1-shutter-driver/>
- [12] DS1023 8-Bit Programmable Timing Element, www.maximintegrated.com/en/products/analog/clock-generation-distribution/DS1023.html
- [13] Michael Lombardi, *The Measurement, Instrumentation, and Sensors Handbook*, Edition: 2nd edition, Chapter: 41 9Time Measurement), Publisher: CRC Press, Editors: John Webster, pp.21, 2014
- [14] Mihai Șerbănescu, Alexandru Achim, Paul Șchiopu, *Control and synchronization system for CETAL-PW laser - delay measurement*, 5th Int.Conf. on

Mathematics and Computers in Sciences and Industry - MCSI 2018, International Symposium - High power lasers applications, August 24- 28 2018, Corfu, Greece

[15] Jerald Graeme, "Photodiode Amplifiers, Op Amp Solutions" – Mc Graw Hill, 1996;

[16] M. Șerbănescu, , Mihaiela Iliescu, Marian Lazar, Calin Ciufudean - *Development of 2D, Ultra-Simple, Low-Cost, Optical Range TOF ScanLaser - Latest Trends in Circuits, Systems, Signal Processing and Automatic Control*, pag 91-96, ISBN: 978-960-474-374-2

[17] Mihaiela Iliescu, Victor Vladareanu, Mihai Serbanescu, Marian Lazar - *Sensor Input Learning for Time-of- Flight Scan Laser*, "Journal of Control Engineering and Applied Informatics, vol19, No.2 pp.51-60, 2017

[18] D. MacFarlane , "Laser beam alignment for ultrashort pulses", *Review of Scientific Instruments*, 62 (8), 1899 - 1903, 1991

[19] M. Anderson, Ward, "All reflective automated beam alignment device for ultrafast lasers", *American Association of Physics Teachers*, doi:10.1119/1.1737398 , 2004

[20] H. Kapteyn and M. Murnane, "Ultrashort light pulses: life in the fast lane", *Physics. World* 12 (1), 31-35, 1999

[21] M. Șerbănescu, M. Pandealea, A. Achim, M. Iliescu – *Command and control system for laser beam position within transmission line at CETAL-PW, UPB Scientific Bulletin, Series A: Applied Mathematics and Physics* 80 (3) 21 (2018);

[22] M. O. Cernaianu, B. De Boisdeffre, D. Ursescu, F. Negoita, C. A. Ur, O. Tesileanu, D. Balabanski, T. Ivanoaica, M. Ciubancan, M. Toma, I. Dancus, S. Gales, "Monitoring and control systems for experiments at ELI-NP, *Romanian Reports in Physics*, Vol. 68, Supplement, P. S349–S443, 2016

[23] Achim Alexandru, Mihai Serbanescu, Aurelian Marcu, Razvan Ungureanu, Gabriel Cojocar, Constantin Diplasu, Georgiana Giubega and Marian Zamfirescu „*CETAL-PW LASER BEAM FAR-FIELD INTENSITY PROFILE IMAGE ANALYSIS*”, TIM2019

[24] Thales Laser – *ATLAS LASER User manual* 051486

[25] Thales Laser – *ISEO User manual* 6801098-108

[26] 74ACT14 Datasheet – *Hex Inverter with Schmitt Trigger Input*, ON Semiconductor

[27] 74ACT132 Datasheet - *Quad 2–Input NAND Schmitt Trigger* , ON Semiconductor

[28] ACPL-061, *Ultra Low Power 10 MBd Digital CMOS Optocoupler*, Avago Technologies

[29] ATMEGA8A Datasheet - *Complete*, www.microchip.com/wwwproducts/en/ATmega8A

Bibliografie

- [30] FT232R Datasheet – FTDI Chip, <https://www.ftdichip.com/Products/ICs/FT232R.htm>
- [31] Raspberry PI 4 – Datasheet - Raspberry Pi Foundation
- [32] LabView - Graphical programming, <https://zone.ni.com/reference/en-XX/help/371361R>
- [33] Groza A, Serbanescu M, Butoi B, Stancu E, Straticiu M, Burducea I, Balan A, Chiroasca A, Mihalcea B, Ganciu M – „Advances in Spectral Distribution Assessment of Laser Accelerated Protons using Multilayer CR-39 Detectors”, *APPLIED SCIENCES-BASEL* 9 (10) 2052 (2019)
- [34] Andreea Groza, AlecsandruChiroasca, ElenaStancu, BogdanButoi, MihaiSerbanescu, Dragana B. Dreghici and Mihai Ganciu – „Assessment of Angular Spectral Distributions of Laser Accelerated Particles for Simulation of Radiation Dose Map in Target Normal Sheath Acceleration Regime of High Power Laser-Thin Solid Target Interaction—Comparison with Experiments”, *APPLIED SCIENCES*. 2020, 10, 4390; doi:10.3390/app10124390
- [35] A. Dubietis et al., “Powerful femtosecond pulse generation by chirped and stretched pulse parametric amplification in BBO crystal”, *Opt. Commun.* 88, 433 (1992)
- [36] TDC502 User Manual Version 2.6 MSC Vertriebs GmbH, <https://www.mtrplus.com/en/downloads-2/download-manuals>
- [37] 74HC14 , Hex inverting Schmitt, trigger https://assets.nexperia.com/documents/data-sheet/74HC_HCT14.pdf
- [38] 74AHC132 Quad 2-input NAND Schmitt trigger, https://assets.nexperia.com/documents/data-sheet/74AHC_AHCT132.pdf
- [39] ELECTRO-OPTIC DEVICE ERX-6, www.eodevices.com/main_erx_6_frameset.htm
- [40] AT90CAN32, Microchip CPU, <http://www.microchip.com/wwwproducts/en/AT90CAN32>
- [41] G. Matras, F. Lureau, S. Laux, O. Casagrande, C. Radier, O. Chalus, F. Caradec F., L. Boudjemaa, C. Simon-Boisson, R. Dabu, F. Jipa, L. Neagu, I Dancus., D. Sporea, C. Fenic and C. Grigoriu, “First Operation above Petawatt with Sub-25”, *Technical Digest (online) (Optical Society of America), paper Tu2C.4*, <https://doi.org/10.1364/HILAS.2014.HTu2C.4>, 2014.
- [42] S.Yu. Mironov, J. Wheeler, R. Gonin, G. Cojocaru, R. Ungureanu, R. Banici, M. Serbanescu, R. Dabu, G. Mourou and E.A. Khazanov / 100 J-level pulse compression for peak power enhancement / *Quantum Electronics* 47 173 (2017)